The Stat6-regulated KRAB domain zinc finger protein Zfp157 regulates the balance of lineages in mammary glands and compensates for loss of Gata-3

Carrie H. Oliver,[1,4] Walid T. Khaled,[1,2,4] Hayley Frend,[1] Jennifer Nichols,[3] and Christine J. Watson[1,5]

[1]Department of Pathology, University of Cambridge, Cambridge CB2 1QP, United Kingdom; [2]Wellcome Trust Sanger Institute, Hinxton, Cambridge CB10 1HH, United Kingdom; [3]The Wellcome Trust Centre for Stem Cell Research, University of Cambridge, Cambridge CB2 1QP, United Kingdom

Lineage commitment studies in mammary glands have focused on identifying cell populations that display stem or progenitor properties. However, the mechanisms that control cell fate have been incompletely explored. Herein we show that zinc finger protein 157 (Zfp157) is required to establish the balance between luminal alveolar pStat5- and Gata-3-expressing cells in the murine mammary gland. Using mice in which the *zfp157* gene was disrupted, we found that alveologenesis was accelerated concomitantly with a dramatic skewing of the proportion of pStat5-expressing cells relative to Gata-3$^+$ cells. This suppression of the Gata-3$^+$ lineage was associated with increased expression of the inhibitor of helix–loop–helix protein Id2. Surprisingly, Gata-3 becomes dispensable in the absence of Zfp157, as mice deficient for both Zfp157 and Gata-3 lactate normally, although the glands display a mild epithelial dysplasia. These data suggest that the luminal alveolar compartment of the mammary gland is comprised of a number of distinct cell populations that, although interdependant, exhibit considerable cell fate plasticity.

[*Keywords*: mammary gland; lineage commitment; Gata-3; transcription; Stat6; progenitors]

Supplemental material is available for this article.

Received November 24, 2011; revised version accepted April 5, 2012.

The mammary gland is unusual in that most development occurs in the adult. At birth, the gland comprises a rudimentary branched structure that elongates and branches during puberty to fill the fat pad. Ducts are comprised of a polarized bilayered epithelium of luminal and basal cells, the latter being primarily differentiated myoepithelium. At the onset of pregnancy, the alveolar lineage arises from progenitors that are stimulated to proliferate and generate lobuloalveolar structures, comprised of luminal and basal cells, which subsequently differentiate to produce milk and are thus essential for survival of the offspring (Hennighausen and Robinson 2005). These distinct epithelial cell types arise from a common multipotent stem cell (Shackleton et al. 2006; Stingl et al. 2006).

Stat5a is essential for mammary gland development during pregnancy and formation of lobuloalveolar structures, as germline deletion of *stat5a* resulted in impaired alveologenesis and lactation failure (Liu et al. 1997). This lactation defect can be rescued in subsequent pregnancies by elevated expression of Stat5b (Liu et al. 1998). Consequently, deletion of both *stat5a/b* genes in mammary epithelium severely impairs alveologenesis (Cui et al. 2004), and this can be rescued by transgenic expression of Stat5a in *stat5a/b*-null mammary cells during pregnancy (Yamaji et al. 2009). The latter study demonstrated that Stat5a is required for the generation and/or expansion of alveolar luminal progenitor cells from mammary stem cells (Yamaji et al. 2009). The Ets transcription factor Elf5 has been suggested to be a master regulator of alveologenesis, as conditional deletion of Elf5 in both luminal and basal cells of the mammary gland resulted in a complete failure to develop the secretory epithelium (Choi et al. 2009). Conversely, overexpression of Elf5 in virgin mammary glands using an inducible transgenic model resulted in precocious alveologenesis and milk secretion (Oakes et al. 2008). This resulted in a diminution in number of luminal progenitor cells that express CD61 (β3 integrin), while in Elf5-null glands, CD61$^+$ luminal progenitor cells accumulated, suggesting a block in differentiation. The connection between Stat5a and Elf5, both downstream targets of prolactin signaling, is not clear. Elf5 has been shown to bind to the proximal *stat5a* gene

[4]These authors contributed equally to this work.
[5]Corresponding author.
E-mail cjw53@cam.ac.uk.
Article is online at http://www.genesdev.org/cgi/doi/10.1101/gad.184051.111. Freely available online through the *Genes & Development* Open Access option.

promoter in late pregnancy, and levels of Stat5a are down-regulated in Elf5-deficient mammary epithelial cells (Choi et al. 2009). However, Stat5a/b-null luminal progenitor cells do not express Elf5, and there are multiple consensus Stat-binding sites in the distal region of the *Elf5* gene promoter (Yamaji et al. 2009), suggesting that there could be a positive regulatory loop between Stat5 and Elf5.

Gata-3, which is expressed in the luminal cells, is required to specify and maintain the differentiation status of luminal epithelial cells (Kouros-Mehr et al. 2006; Asselin-Labat et al. 2007). Conditional deletion of Gata-3 during gestation resulted in detachment of cells from the basement membrane, resulting in cell death and lactation failure (Kouros-Mehr et al. 2006). $CD61^+$ luminal progenitors also accumulated in Gata-3-null mammary glands (Asselin-Labat et al. 2007). Stat6 and IL-4/IL-13 are upstream regulators of Gata-3, and these signaling molecules are required for efficient lobuloalveologenesis, as there was a considerable delay in proliferation and differentiation in the absence of Stat6 or IL-4/IL-13 (Khaled et al. 2007). A microarray analysis of 5-d-gestation (5dG) mammary tissue revealed that the most up-regulated transcript in *stat6*$^{-/-}$ tissue was a previously undescribed gene, *zinc finger protein 157* (*zfp157*). In this study, we explore the function of Zfp157 in alveologenesis and reveal that this transcriptional regulator controls the balance of luminal populations and is a critical mediator of Gata-3 signaling.

Results

Zfp157 is a Stat6-regulated KRAB domain zinc finger protein

The domains of Zfp157 are commensurate with it being a member of the family of Krüppel-associated box (KRAB) domain-containing zinc finger proteins (Fig. 1A; Urrutia 2003). This notion is further supported by the nuclear localization of Zfp157, where it is present in distinct puncta (Fig. 1B). Zfp157 is expressed in multiple tissues in mice both during embryogenesis and in the adult (CH Oliver, unpubl.). KRAB zinc finger proteins are transcriptional repressors that act by binding DNA and recruiting Kap1 via the KRAB domain. Kap1 in turn recruits a complex of heterochromatin remodeling proteins to silence nearby chromatin (Urrutia 2003). To determine whether Zfp157 is differentially expressed between the luminal and basal cells, quantitative RT–PCR (qRT–PCR) was performed on FACS-sorted luminal and basal cell populations from *stat6*$^{-/-}$ and strain-matched wild-type controls. We observed no difference in Zfp157 expression in virgin glands, as expected from the paucity of pStat6-expressing cells at this stage of development (Khaled et al. 2007), but at 5dG, there was a significant increase in expression in both the luminal and basal cell populations in the *stat6*$^{-/-}$ glands, with a more substantial increase in the basal cells (Fig. 1C). The luminal cell population can be further divided by sorting on the basis of CD49b and Sca1 expression (Li et al. 2009). Zfp157 is expressed in both subpopulations, although in the absence of Stat6, expression is highest in the Sca1 low cells (Fig. 1D). It is worth noting that although the number of luminal progenitors in the *stat6*$^{-/-}$ mice increased (Supplemental Fig. S1a), their proliferative potential was diminished when assayed in culture (Supplemental Fig. S1b). Such accumulation of progenitors is reminiscent of the phenotype observed in the absence of *gata-3* (Asselin-Labat et al. 2007).

To investigate how Zfp157 and pStat6 interact, we examined the promoter region of *zfp157* and identified two putative Stat6-binding sites and also a Gata3 site. A chromatin immunoprecipitation (ChIP) analysis revealed Stat6 occupancy of the *zfp157* promoter (Fig. 1E) and more proximal Gata-3 binding (Supplemental Fig. S2a). Although both are putative transcriptional activators, some repressor activity has been reported (Takaki et al. 2008; Ray et al. 2009). Consistent with our data, we suggest that pStat6 and Gata-3 repress *zfp157* expression. To test this, mammary epithelial cells were treated with IL-4, and the expression of *zfp157* was measured by qRT–PCR. As expected, *zfp157* expression was decreased 24 h after treatment (Supplemental Fig. S2b). This was further supported by analysis of *zfp157* expression in conditional Gata-3 knockout glands, where we found slightly elevated expression (Supplemental Fig. S2c). Taken together, these data strongly suggest that Stat6 and Gata-3 repress the transcription of *Zfp157* to promote timely alveologenesis.

Zfp157 is expressed throughout adult mammary gland development

We examined the expression of *zfp157* during all stages of adult mammary gland development by qRT–PCR (Fig. 1F) and observed that expression increases during pregnancy and throughout involution, while only low levels were detectable in the virgin and lactating glands. The pattern of *zfp157* expression is commensurate with a role in regulating alveologenesis, and to investigate this further, we generated a functional knockout/reporter mouse using embryonic stem cells in which the *β-galactosidase* gene had been inserted into the *zfp157* locus (Supplemental Fig. S3; Skarnes et al. 2004). Since the insertion contains a splice acceptor site and a stop codon and is located toward the 5′ end of the gene, it was expected that no functional protein would be produced, as the zinc finger motifs would be deleted. This was confirmed using qRT–PCR, as no full-length transcript was detectable in homozygous animals, while, interestingly, heterozygous mice had diminished expression (Supplemental Fig. S3d). The lacZ reporter was detected during embryogenesis in the developing mammary placodes. Expression was further detected in a proportion of basal cells in both alveoli and ducts of the mature adult gland, with a few luminal cells also staining blue (Fig. 1G). Immunofluorescence (IF) analysis of CK14 and CK18 in sections of *zfp157*$^{lacZ/+}$ and *zfp157*$^{lacZ/lacZ}$ glands showed that there are no morphological changes when Zfp157 is depleted and that the basal layer is intact (Supplemental Fig. S4). Thus, we can conclude that Zfp157 is predominantly expressed in CK14-expressing cells. Since Stat6 is primarily detected in luminal mammary

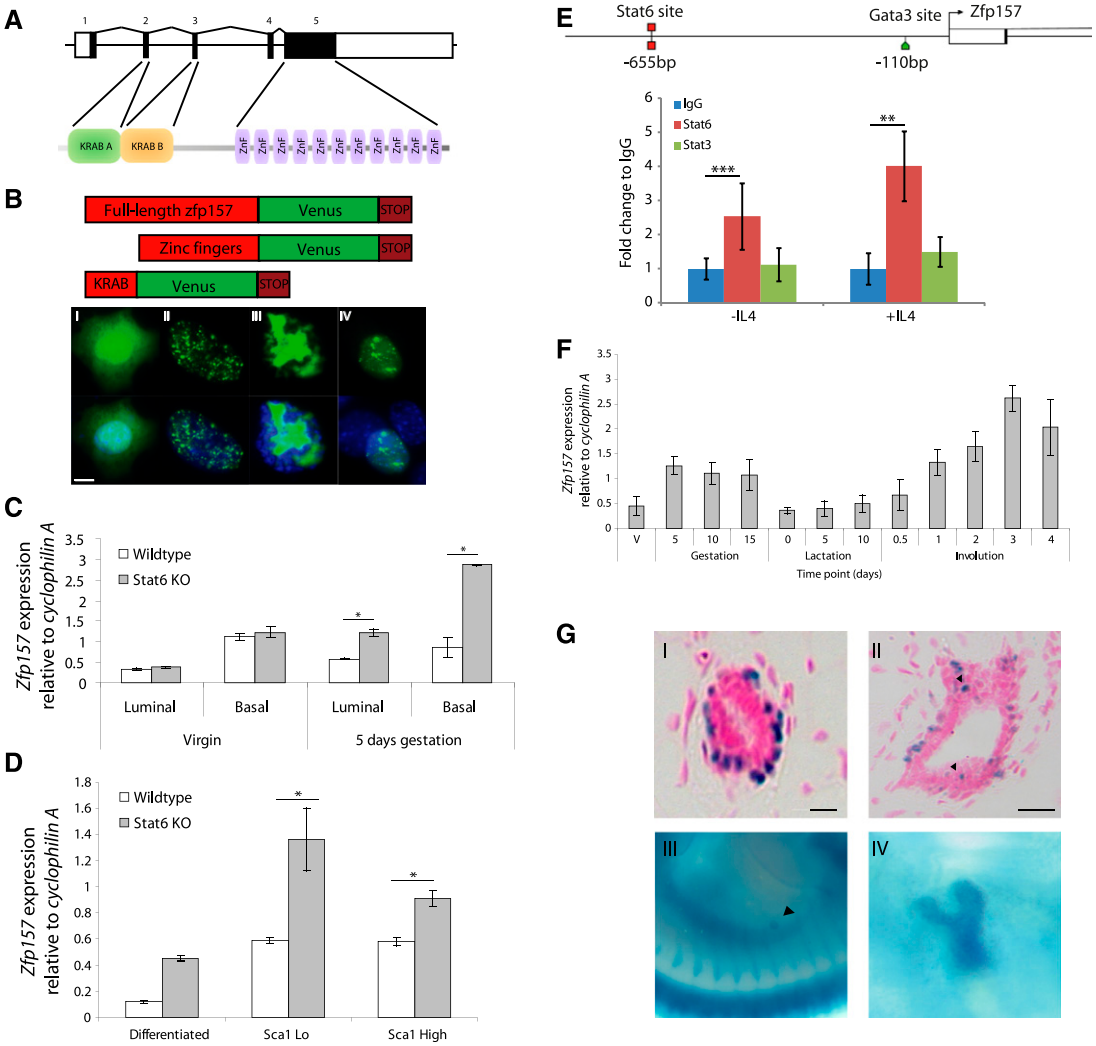

Figure 1. Zfp157 is a nuclear protein that is regulated by Stat6 and is expressed predominantly in basal mammary epithelial cells. (*A*) Schematic representation of *zfp157*-encoding exons and domains. (*B*) *zfp157* was cloned and tagged with a Venus tag and transfected into NIH-3T3 cells. Control vector shows diffuse staining throughout the cell, whereas Zfp157-Venus locates to the nucleus and exhibits a punctate pattern of staining characteristic of Krab-containing zinc finger proteins. Constructs with just the zinc finger motifs or just the Krab domains were also designed and transfected into NIH-3T3 cells. Both of these localize to the nucleus, but the discreet pattern of foci is lost. (*C*) qRT–PCR of *zfp157* expression relative to cyclophilin A in mammary cells sorted into luminal and basal populations in wild-type and *stat6*$^{-/-}$ (knockout [KO]) mice. Values represent means ± SD; $n = 3$. (*) $P < 0.05$. (*D*) The luminal cell population was further sorted based on CD49b and Sca1 expression to identify the luminal progenitor populations. Values represent means ± SD; $n = 3$. (*) $P < 0.05$. (*E*) ChIP analysis was performed on a putative Stat6-binding site upstream of the *zfp157* transcriptional start site. Stat6 was found to preferentially bind to this site, and binding was increased in the presence of IL-4. Both nonspecific IgG and Stat3 antibodies were used as negative controls. (***) $P < 0.001$; (**) $P < 0.01$. (*F*) qRT–PCR analysis of *zfp157* expression throughout a mammary gland developmental time course. Values represent means ± SD. (*G*) Detection of Zfp157-lacZ expression using X-gal staining in heterozygous mice. Sections are counterstained with nuclear fast red. Alveoli (panel *I*) and ducts (panel *II*) show basal cells and rare luminal cells expressing the transgene. Bar, 50 μm. (Panel *III*) Expression in the developing mammary placodes is seen in the embryo. Image taken from an embryonic day 11.5 (E11.5) embryo. The arrowhead indicates placode number 3. (Panel *IV*) Expression is still observed in the rudimentary mammary gland at E16.5 just after the first bifurcation of the primary duct.

epithelial cells, this could explain why Zfp157 expression is rarely found in this compartment.

Deletion of Zfp157 reveals roles in alveologenesis

Next, we examined the consequences of Zfp157 deletion during puberty. At 5 wk of age, the terminal end buds (TEBs) at the leading edge of the gland have just reached the lymph node in the control animals. In the *zfp157*$^{lacZ/lacZ}$ glands, the TEBs had significantly passed this point (Supplemental Fig. S5), as quantified by measuring the distance of TEB migration from the center of the lymph node. There was no observable difference between the genotypes at 8 wk of age when the gland has completely filled the fat

pad, suggesting that Zfp157 affects only the rate of ductal elongation (Fig. 2A).

Since *stat6*$^{-/-}$ mice display delayed alveologenesis during pregnancy (Khaled et al. 2007), we postulated that *zfp157*$^{lacZ/lacZ}$ mice would exhibit precocious alveologenesis. To this end, 8- to 10-wk-old virgin mice were mated and sacrificed at 5dG, 10dG, and 15dG. Whole-mount analysis revealed increased alveolar density in the *zfp157*$^{lacZ/lacZ}$ animals at all stages, but most notably at 5dG (Fig. 2A). Quantification using hemotoxylin and eosin (H&E) sections (Supplemental Fig. S6) revealed an increased number of alveoli per square millimeter at all stages examined (Fig. 2B), with the most marked difference occurring at 5dG. As anticipated, this is the opposite phenotype to *stat6*$^{-/-}$ mice, which express increased levels of Zfp157, suggesting that Zfp157 is the critical downstream target of Stat6.

Since accelerated alveologenesis should be accompanied by elevated proliferation, sections from mammary glands at 5dG, 10dG, and 15dG were stained for Ki67, a marker of proliferation (Fig. 2C). A significant increase in the number of actively proliferating cells was observed at 5dG in the *zfp157*$^{lacZ/lacZ}$ mice (Fig. 2D) but not subsequently, suggesting that Zfp157 is important in early pregnancy when the alveolar lineages are being established. No effect on mammary gland development was observed in lactation or involution (Supplemental Fig. S7).

Zfp157 is a master regulator of lineage commitment

We next sought to establish the mechanism of accelerated alveologenesis by examining the expression of a number of candidate proteins that have been shown previously to be essential for alveologenesis. One such protein is Gata-3, itself a target of Stat6 and shown to be an essential regulator of luminal cell differentiation and survival (Kouros-Mehr et al. 2006; Asselin-Labat et al. 2007). To examine any changes in Gata-3 expression, we used IF to determine the number of Gata-3-expressing cells and found that there were, on average, less Gata-3 cells per alveolus or duct in the *zfp157*$^{lacZ/lacZ}$ sections (Fig. 3A). Gata-3 has been reported to function with ERα (Kouros-Mehr et al. 2006). Although ERα-expressing cells do not proliferate, they are essential for alveologenesis to occur, as they signal in a paracrine fashion to ERα-negative cells. IF on 5dG samples confirmed that ERα and Gata-3 are coexpressed in normal mammary cells (Supplemental Fig. S8a) and in *zfp157*$^{lacZ/lacZ}$ mammary glands (data not shown), and thus we would envisage a decrease in the number of ERα cells in the absence of Zfp157, which is indeed the case (Fig. 3B). Progesterone receptor (PR)-expressing cells are also required for alveologenesis (Conneely et al. 2007) and are reported to coexpress with ERα (Booth and Smith 2006), which we confirmed by co-IF (Supplemental Fig. S8b). Therefore, we would also predict a decrease in the number of PR$^+$ cells, and there are indeed fewer PR$^+$ cells in the absence of Zfp157 (Fig. 3C). We conclude that the number of cells that express Gata-3/ERα/PR is reduced in the *zfp157*$^{lacZ/lacZ}$ mammary glands at 5dG.

With the number of cells coexpressing these three key alveologenesis regulators diminished, it follows that another cell population must be expanded. Since pStat5 is a downstream mediator of the prolactin signaling pathway and is required for expansion of alveolar progenitors and alveologenesis (Liu et al. 1997; Yamaji et al. 2009), we determined the number of pStat5 expressing cells. As anticipated, *zfp157*$^{lacZ/lacZ}$ mammary glands displayed a dramatically higher number of pStat5-positive cells (Fig. 3D). Despite this, the total levels of Stat5a were not changed, as assessed by immunoblot (Supplemental Fig. S9a). Interestingly, in the *zfp157*$^{lacZ/lacZ}$ glands, Stat5a has a predominantly nuclear localization, while in the *zfp157*$^{lacZ/+}$ glands, Stat5a is also found in the cytosol (Supplemental Fig. S9B). However, this up-regulation of Stat5 activation is not associated with a change in the level of Elf5 or the prolactin receptor (Supplemental Fig. S9c,d). Furthermore, expression of the milk protein gene WAP is considerably reduced in *zfp157*$^{lacZ/lacZ}$ glands, suggesting that the pStat5-positive cells are undifferentiated luminal progenitors (Supplemental Fig. S9e; Yamaji et al. 2009).

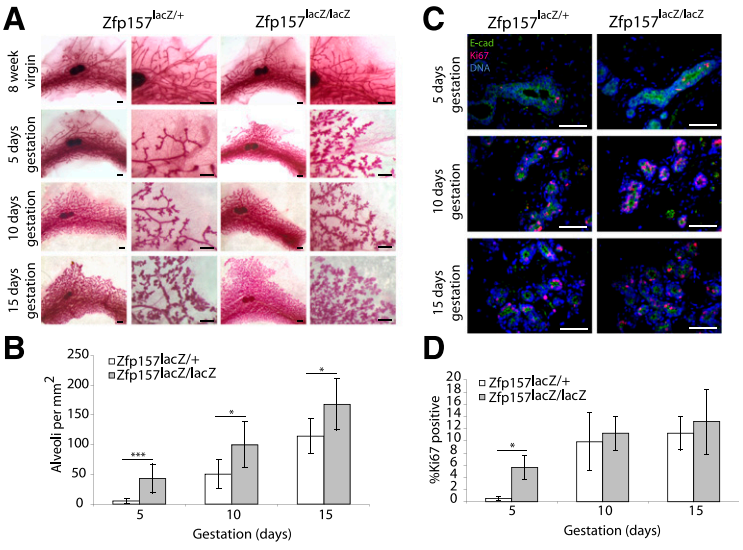

Figure 2. Ablation of Zfp157 results in accelerated alveologenesis and elevated levels of proliferation. (*A*) Representative whole mounts of mammary glands from 8-wk-old virgin *zfp157*$^{lacZ/lacZ}$ and *zfp157*$^{lacZ/+}$ mice and 5dG, 10dG, and 15dG mice. Whole mounts are stained with carmine red. Bar, 1 mm. $n = 5$. (*B*) The number of alveoli per square millimeter was counted from H&E sections. Values represent means ± SD; $n = 3$. (*) $P < 0.05$; (***) $P < 0.001$. (*C*) Representative images of IF for Ki67 (red) at three gestation time points. $n = 3$. (*D*) The percentage of Ki67-positive cells was calculated from five random images per gland. Values represent means ± SD; $n = 3$. (*) $P < 0.05$.

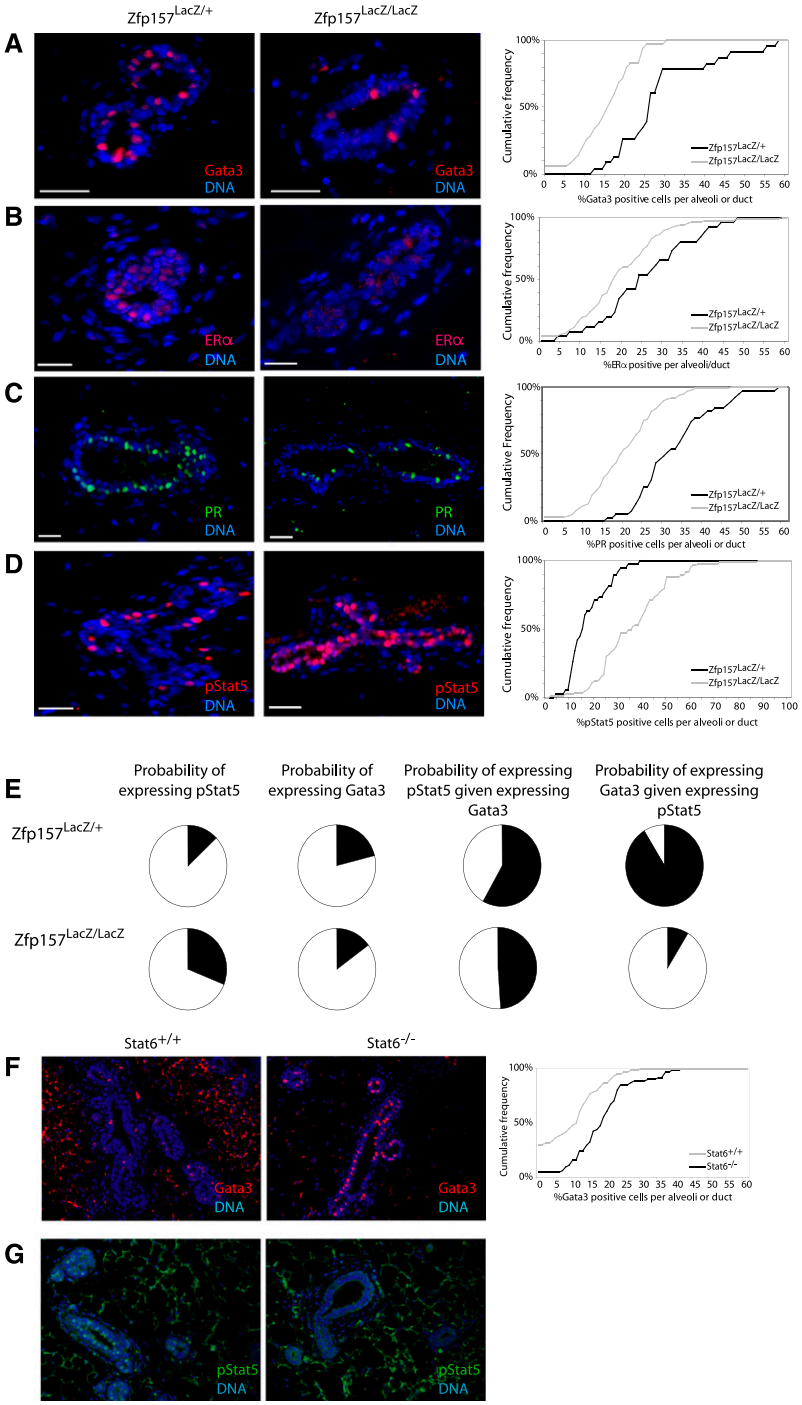

Figure 3. Zfp157 controls the proportions of alveolar subpopulations. (*A*) IF for Gata-3 in 5dG mammary glands shows decreased numbers of positive cells in *zfp157*$^{lacZ/lacZ}$ glands compared with *zfp157*$^{lacZ/+}$ glands. Quantification by counting individual cells was carried out and plotted as a cumulative frequency diagram. Data from *zfp157*$^{lacZ/lacZ}$ mice show a significant shift to the left as less cells per alveolus or duct express Gata-3 ($n = 3$; $P < 0.05$). (*B*) IF for ERα at 5dG reveals a reduced number of positive cells in the *zfp157*$^{lacZ/lacZ}$ glands compared with the control *zfp157*$^{lacZ/+}$. Quantification was carried out by counting the number of positive cells per alveolus or duct and was plotted as a cumulative frequency diagram. *zfp157*$^{lacZ/lacZ}$ glands show a significant decrease in the average number of positive cells compared with *zfp157*$^{lacZ/+}$ glands, as shown by a shift to the left ($n = 3$; $P < 0.05$). (*C*) IF for PR in 5dG glands shows a reduced number of PR-expressing cells in *zfp157*$^{lacZ/lacZ}$ glands compared with *zfp157*$^{lacZ/+}$controls. Counting of the number of positive cells per alveolus or duct reveals a significant decrease in the *zfp157*$^{lacZ/lacZ}$ glands ($n = 3$; $P < 0.05$). (*D*) IF for pStat5 shows a dramatic increase in the number of pStat5-expressing cells in the *zfp157*$^{lacZ/lacZ}$ glands at 5dG. Quantification of the number of positive cells per alveolus or duct reveals a dramatic increase in the average number of positive cells ($n = 3$; $P < 0.05$). (*E*) Graphical representations of the probability of a cell expressing either pStat5, Gata-3, or pStat5 given it expresses also Gata-3 or vice versa. (*F*) IF for Gata-3 expression in Stat6$^{-/-}$ mice and controls. Stat6$^{-/-}$ glands show a significantly higher number of Gata-3-expressing cells ($n = 3$; $P < 0.05$). (*G*) IF for pStat5 in Stat6$^{-/-}$ mice. Expression of pStat5 is absent at 5dG when Stat6 is also ablated ($n = 3$).

We then sought to clarify the relationship between these populations and the proliferating population of cells. Those expressing ERα, PR, and Gata-3 were not proliferative, as expected (Supplemental Fig. S10a), and although some pStat5^{+}/PCNA^{+} cells were observed, the majority of pStat5-expressing cells do not appear to be proliferating either (Supplemental Fig. S10b). This was unexpected, as Stat5 has been associated with proliferation (Miyoshi et al. 2001; Cui et al. 2004). We then tested whether Gata-3 and pStat5 coexpress using IF, and it became apparent that there is a mix of single-positive and double-positive cells present in the normal mammary gland (Supplemental Fig. S11). To quantify these populations, cells in a random selection of alveoli and ducts were counted and scored as either negative or positive for either Gata-3 or pStat5 or both. These data were subsequently analyzed to provide the probability of a cell expressing a given transcription factor (Fig. 3E). In the normal gland, any cell has a 13% probability of expressing pStat5 and a 21% chance of expressing Gata-3. The probability that a Gata-3^{+} cell will also

have pStat5 is ~58%. Conversely, the probability that a pStat5$^+$ cell will also express Gata-3 is 88%. This suggests that most pStat5-positive cells in the normal mammary gland also express Gata-3, whereas about half of Gata-3 cells do not express pStat5. To investigate how these frequencies change in the absence of Zfp157, this analysis was repeated on *zfp157*$^{lacZ/lacZ}$ sections. The probability of a cell expressing Gata-3 had halved from 21% to 9%, while the probability of being a pStat5$^+$ cell had more than doubled from 13% to 31%. The probability of a Gata-3-expressing cell being positive also for pStat5 was remarkably unchanged, dropping from 58% to 49%. Strikingly, the probability of a pStat5$^+$ cell being also Gata3$^+$ decreased from 88% to only 15%. This reveals a dramatic shift in the cellular composition of the mammary gland in the absence of Zfp157: The population of cells expressing only pStat5 has dramatically expanded at the expense of the double-positive Gata-3$^+$/pStat5 cells, which are now a very minor component. It is possible that these double-positive cells are alveolar progenitors that subsequently commit to either a Gata-3$^+$ or pStat5$^+$ lineage. However, FACS analysis using CD61 or Sca1 and colony assays did not reveal any significant differences in either virgin or 5dG glands (Supplemental Fig. S12), suggesting that these double-positive cells could be either earlier in the hierarchy or a separate differentiated lineage that is currently not detectable using standard FACS methods.

Given that the *stat6*$^{-/-}$ mice display the opposite phenotype to the *zfp157*$^{lacZ/lacZ}$ mice and have increased levels of *zfp157* expression, we were interested in examining the cell populations in *stat6*$^{-/-}$ mice. As expected, the number of Gata-3-expressing cells was increased (Fig. 3F). These also expressed ERα and PR, so this population was increased in the presence of elevated Zfp157 expression (Supplemental Fig. S13). Remarkably, the number of pStat5$^+$ cells was not only reduced, but entirely absent (Fig. 3G). While factors other than increased expression of *zfp157* are no doubt important, it does appear that Zfp157 plays a major role in the phenotypic effects of Stat6 depletion. The phenotype at 5dG of reduced alveologenesis observed in *stat6*$^{-/-}$ mice does not persist until 15dG, when levels of *zfp157* expression return to normal (data not shown), possibly as a consequence of Gata-3 up-regulation, which compensates for the absence of Stat6 and represses expression of *zfp157*.

Gata-3 is not essential for alveologenesis when Zfp157 is absent

On the basis of the diminished population of Gata-3 cells, we hypothesized that in *zfp157*$^{lacZ/lacZ}$ mammary glands, Gata-3 may become dispensable for alveologenesis. Previous work has shown that if Gata-3 is deleted during late pregnancy, mammary epithelial cells die, resulting in failed lactation (Kouros-Mehr et al. 2006; Asselin-Labat et al. 2007). To investigate whether deleting Zfp157 did indeed render Gata-3 superfluous, we generated *zfp157*$^{lacZ/lacZ}$;*gata3*$^{fl/fl}$;*BLG-Cre* mice. To confirm that our Gata-3 knockout model reflects previously published data, *gata3*$^{fl/fl}$;*BLG-Cre* females were mated and allowed to litter. Pups nursed by *gata3*$^{fl/fl}$;*BLG-Cre* dams had less milk in their stomachs and showed signs of severe dehydration 1 or 2 d after birth and were euthanized at this time. Examination of the glands by whole mount and H&E revealed very few expanded alveoli (Fig. 4A). In contrast, pups nursed by *zfp157*$^{lacZ/lacZ}$;*gata3*$^{fl/fl}$;*BLG-Cre* dams gained weight normally, albeit slightly more slowly for some litters (Fig. 4B). Examination at 10 d lactation revealed glands fully populated with alveoli with some small areas of regression (Fig. 4C), possibly due to later deletion of the *gata3* alleles. We confirmed expression of WAP and pStat5 in double-knockout glands by Western blot (Fig. 4D). This rescue of lactation failure shows that Gata-3 is not required as a survival signal or mediator of alveologenesis, provided Zfp157 is not expressed.

Survival of Gata-3-deleted cells is associated with epithelial dysplasia

Examination of the mammary glands of *zfp157*$^{lacZ/lacZ}$;*gata3*$^{fl/fl}$;*BLG-Cre* dams by H&E revealed signs typical of a mild epithelial dysplasia in all ducts and alveoli (Fig. 4E). The alveoli show an increased number of binucleate cells in which the nuclei are no longer in their typical basal localization, but are instead frequently located toward the apical surface of the cell. Furthermore, the cells in the alveoli and ducts are of variable size. While no tumors developed in the short time period examined, it is not unreasonable to hypothesize that these mice may develop breast tumors after multiple rounds of pregnancy or later in life. GATA-3 is considered a good prognostic factor for breast cancer (Mehra et al. 2005). However, our data show that loss of Zfp157 in the mouse mammary gland obviates the need for Gata-3, and so it is possible that breast cancers with a poor prognosis and GATA-3 expression have instead lost ZNF157, the putative human homolog of Zfp157.

Precocious expression of the transcriptional repressor Id2 in Zfp157$^{lacZ/lacZ}$ *tissue*

To elucidate the mechanism by which Zfp157 controls lineage specification, we focused on inhibitor of DNA-binding 2 (Id2), which has been shown to be essential for alveologenesis and lactation (Mori et al. 2000) and for proliferation of mammary epithelial cells downstream from receptor activator of NF-κB ligand (RANKL) (Kim et al. 2006) and is regulated by Stat5a in virgin animals in response to E+P treatment (Santos et al. 2010). Levels of Id2 mRNA were increased in *zfp157*$^{lacZ/lacZ}$ mammary glands at 5dG (Fig. 5A). Id2 function is regulated by nuclear translocation, and examination of nuclear/cytoplasmic fractions prepared from 5dG tissues by immunoblot showed an increase in Id2 protein levels in both the cytoplasmic and nuclear compartments (Fig. 5B). *Id2* mRNA expression has been shown to be increased around 14dG (Mori et al. 2000). However, in *zfp157*$^{lacZ/lacZ}$ mammary glands, elevated expression of Id2 is observed at 5dG, much earlier than in controls (Fig. 5C). Thus, we can conclude that the accelerated alveologenesis observed in the absence of Zfp157 is at least in part due to an increase in the number of pStat5$^+$ cells and associated elevation of Id2 expression and activity.

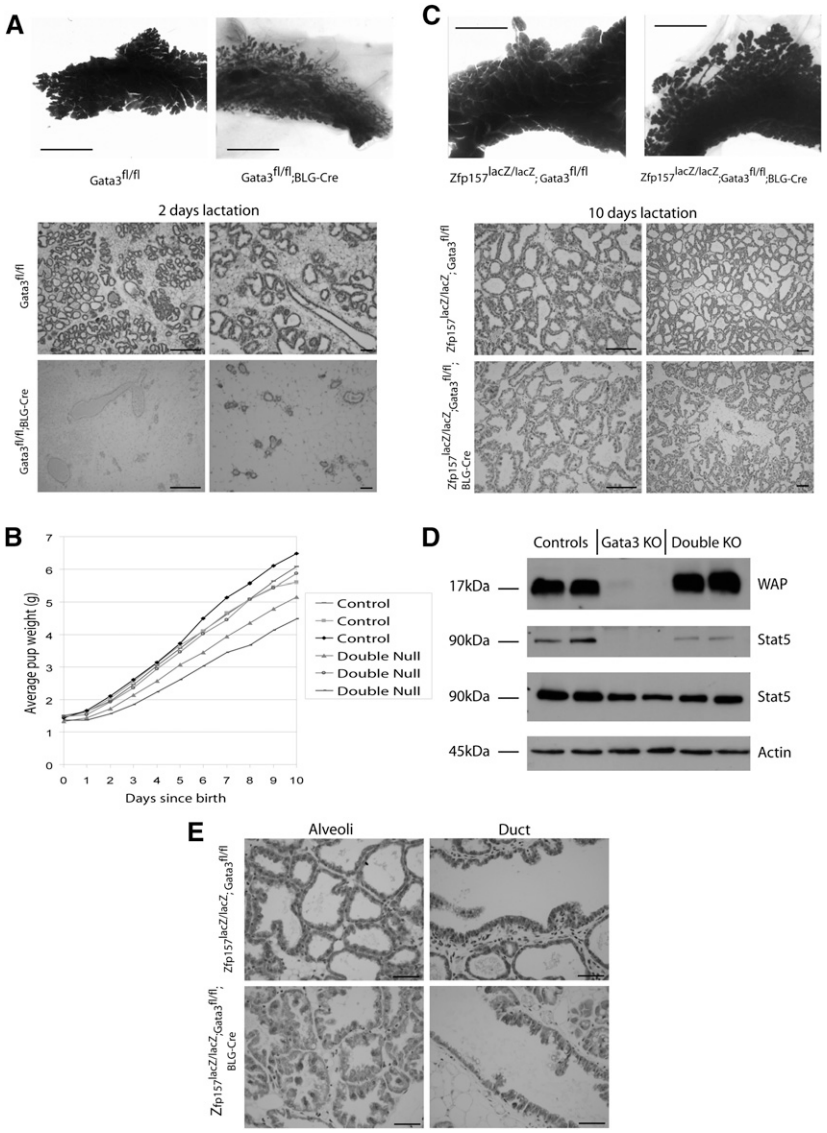

Figure 4. Lactation failure in *gata3*$^{fl/fl}$*;BLG-Cre* mice is rescued by ablation of Zfp157. (*A*) Representative whole mounts and H&E sections from control *gata3*$^{fl/fl}$ and *gata3*$^{fl/fl}$*;BLG-Cre* mice at 2 d of lactation. *gata3*$^{fl/fl}$*;BLG-Cre* mice display regressed alveoli and lactation failure ($n > 3$). Bars: whole mount, 1 mm; section, 50 μm. (*B*) Average weight of pups nursed by control dams (*zfp157*$^{lacZ/lacZ}$) and dams doubly null for Gata-3 and Zfp157 (*zfp157*$^{lacZ/lacZ}$*;gata3*$^{fl/fl}$*;BLG-Cre*). No significant difference between the two groups was observed, and although some pups nursed by double-null dams displayed a lower average weight, all thrived ($n = 3$). (*C*) Representative whole mounts and H&E sections from control and *zfp157*$^{lacZ/lacZ}$*;gata3*$^{fl/fl}$*;BLG-Cre* glands at 10 d of lactation shows expanded alveoli with only small areas of regression ($n > 3$). Bars: whole mount, 1 mm; section, 50 μm. (*D*) Western blot analysis of WAP and pStat5 levels in mammary gland extracts from control (*gata3*$^{fl/fl}$), Gata-3 knockout (Gata-3 KO) (*gata3*$^{fl/fl}$*;BLG-Cre*), and double-knockout (Double KO) (*zfp157*$^{lacZ/lacZ}$*;gata3*$^{fl/fl}$*;BLG-Cre*) mice. Actin was used as a loading control ($n = 2$). (*E*) *zfp157*$^{lacZ/lacZ}$*;gata3*$^{fl/fl}$*;BLG-Cre* glands at 10 d of lactation display signs of mild epithelial dysplasia in both the alveoli and ducts. Bar, 50 μm.

We present a hypothetical model of the mode of action of Zfp157 (Fig. 5D). Basally located multipotent progenitors express Zfp157, which represses proliferation of these progenitors. In response to the hormones of pregnancy, progenitor cells divide and exit the niche to give rise to a bipotent luminal daughter cell that transiently expresses Zfp157. IL-4 and IL-13 induce phosphorylation of Stat6, which in turn induces expression of Gata-3, and these coordinately repress Zfp157 expression. In the absence of Zfp157, Stat5 now becomes phosphorylated to yield a double-positive cell, which subsequently divides to generate daughter cells that are either Gata-3- or pStat5-positive. pStat5 induces the expression of Id2, which leads to proliferation. If Zfp157 is deleted, the pStat5 population is unrestrained, resulting in increased proliferation, and Gata-3 cells become scarce, as they are no longer required. The counterpoint of this is that without Gata-3 to repress Zfp157, alveologenesis fails, as pStat5 cells are no longer extant.

Discussion

A number of transcription factors have been shown to regulate commitment of progenitor cells to the mammary alveolar luminal lineage, including Stat5a, Elf5, Gata-3, and Stat6. Previous studies have shown that the Gata-3- and Elf5-expressing cells are distinct subpopulations (Oakes et al. 2008) and that Gata-3 and ERα colocalize (Kouros-Mehr et al. 2006). However, the mechanism that determines commitment to either one of these lineages has not been determined. Gata-3 is a target of the IL-4/IL-13/Stat6 pathway, which we showed previously to be important in controlling proliferation and differentiation of alveolar progenitors during early pregnancy (Khaled et al. 2007). In addition to being a transcriptional activator, Stat6 can function also as a repressor, and a microarray analysis of *stat6*$^{-/-}$ mammary tissue at 5dG revealed that expression of *zfp157* is highly up-regulated in the absence of Stat6.

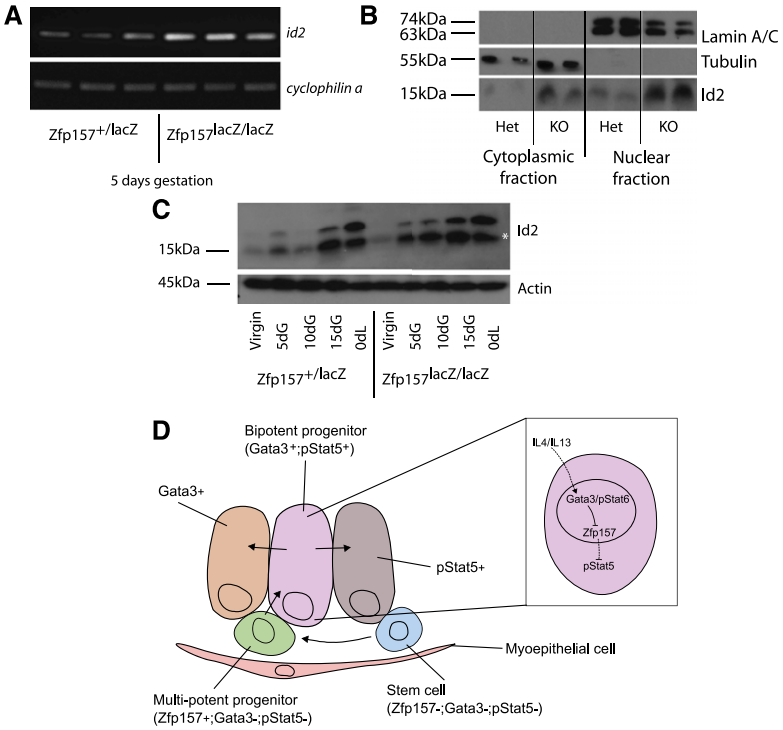

Figure 5. Expression and nuclear localization of Id2 is regulated by Zfp157. (*A*) PCR for Id2 expression shows increased levels in $zfp157^{lacZ/lacZ}$ mammary glands at 5dG ($n = 3$). (*B*) Western blot analysis of 5dG glands after nuclear/cytoplasmic fractionation shows elevated levels of Id2 in both the nucleus and the cytoplasm ($n = 5$). Lamin A/C and tubulin were used as loading controls for the nuclear and cytoplasmic fractions, respectively. (*C*) Western blot analysis shows that Id2 levels increase during gestation. This increase occurs 5–10 d earlier in the $zfp157^{lacZ/lacZ}$ mammary glands ($n = 3$). The Id2 band is marked with an asterisk. (*D*) Proposed model showing Zfp157 expression in a basal multipotent progenitor cell that gives rise to a bipotent daughter cell that is positive for both Gata-3 and pStat5. This cell, which will be transiently positive for Zfp157, can divide to give rise to either a Gata-3-positive cell or a pStat5-positive cell. In response to IL4/IL13 signaling, Stat6 becomes phosphorylated and upregulates expression of Gata-3, and both of these transcription factors suppress expression of Zfp157, which is itself a repressor of pStat5. In turn, expression of Id2 is elevated, which increases proliferation.

Zfp157 is a member of a family of transcriptional repressors that modify chromatin structure

The structure of Zfp157 reveals that it is a KRAB domain-containing zinc finger transcription factor (KRAB-ZFP) that is expressed in the embryonic placode and the adult gland throughout a mammary developmental cycle, with higher levels during gestation and late involution (Fig. 1). Expression is higher in the basal cells. This reflects its suppression by Stat6, which is expressed in luminal cells, and by Gata-3 and IL-4. KRAB-ZFPs comprise the largest family of transcription factors in the mammalian genome, although their functions and target genes are not well understood. It is thought that KRAB-ZFPs bind to DNA and recruit corepressors such as KAP1, HDACs, HP1, and Setdb1 to silence gene expression from target promoters (Urrutia 2003). Recently, it has been shown that ZNF431 (the human homolog of Zfp431) directly represses expression of Patched 1, a target of Hh signaling (He et al. 2011). It can be anticipated that Zfp157 modulates the expression of Stat6 and Gata-3 target genes in the subpopulation of alveolar cells in which these transcription factors are expressed. Our data also suggest that expression of Zfp157 needs to be extinguished to allow proliferation of alveolar progenitors.

Zfp157 has a transient role in ductal elongation

In order to determine the function of Zfp157, we generated mice that expressed a lacZ reporter construct from the endogenous *zfp157* locus to produce a fusion protein with the KRAB domains, producing also a functional knockout. In the mammary glands of young virgin animals, ductal elongation was accelerated by deletion of Zfp157, but this difference did not persist and there was no overt difference between knockout and control glands by 8 wk of age (Fig. 2A). However, alveologenesis was accelerated in $zfp157^{lacZ/lacZ}$ glands during gestation (Fig. 2 A,B), and this was accompanied by an approximately eightfold increase in the percentage of proliferating cells at 5dG (Fig. 2C,D).

Zfp157 controls the balance of alveolar luminal subpopulations

Given the established roles for Gata-3 and Stat5 in establishing and maintaining cells of the alveolar lineage and the distinct expression patterns of Gata-3 and the Stat5 target Elf5 (Oakes et al. 2008), we used IF to investigate the relative proportions of these different populations of cells in both the presence and absence of Zfp157 and Stat6. First, we observed that the number of cells expressing Gata-3 was decreased in $zfp157^{lacZ/lacZ}$ glands compared with heterozygous controls (Fig. 3A). A similar decrease was observed for ERα and PR, which are coexpressed with Gata-3 (Fig. 3B,C). Conversely, more cells express Gata-3 in $stat6^{-/-}$ tissue (Fig. 3F). This could suggest that Zfp157 is required for either the commitment of the Gata-3-expressing lineage from progenitors or the survival of Gata-3-expressing cells. The latter seems unlikely, since Gata-3 suppresses the expression of Zfp157. A striking increase in the number of pStat5-positive cells was elicited by deletion of Zfp157 (Fig. 3D), and perhaps even more remarkable is the complete loss of pStat5 cells in the $stat6^{-/-}$ glands (Fig. 3G). The implication of these results is that Stat6 controls the levels of Zfp157, which in turn suppresses Stat5 activation, and that the balance of cell types is controlled by the absolute amounts of Zfp157. Co-IF for pStat5 and Gata-3 identified three populations of cells: Gata-3$^+$, pStat5$^+$, and Gata-3/

pStat5 double positive (Supplemental Fig. S8). Approximately half of all Gata-3$^+$ cells are also pStat5$^+$. In *zfp157*$^{lacZ/LacZ}$ mammary glands, the most dramatic change is in the pStat5$^+$ population, which has massively expanded, resulting in very few double-positive cells. Probability calculations revealed a remarkable skew in the probability that a pStat5-expressing cell will also be a Gata-3-expressing cell when Zfp157 is not expressed, changing from 88% to 15% (Fig. 3E). A consequence of this is that the double-positive cells are severely depleted. It is currently not clear whether these are earlier progenitors or a distinct differentiated lineage. Additional markers of these lineages will be required to solve this question.

Lactation defect in Gata-3 conditional knockout mice is rescued by Zfp157 deletion

The appearance of a substantial population of cells that are independent of Gata-3 raised the question of whether Gata-3 is still required for alveologenesis in the absence of Zfp157 expression. Conditional deletion of Gata3 using the BLG promoter to drive Cre expression in luminal alveolar cells resulted in lactation failure, as previously found using the WAP promoter (Fig. 4A). Strikingly, this lactation failure was completely rescued by coincident deletion of Zfp157. Alveologenesis proceeded normally, resulting in milk secretion, as evidenced by the growth of pups nursed by *zfp157*$^{lacZ/lacZ}$;*gata3*$^{fl/fl}$;*BLG-Cre* dams, expression of WAP, and histological sections showing expanded alveoli (Fig. 4B,C). Occasional areas of regression could reflect clonal expansion of cells that undergo late recombination and, consequently, cell death (Kouros-Mehr et al. 2006). Close inspection of H&E sections revealed elongated luminal cells that were frequently binucleate and exhibited apical localization of the nuclei, indicative of mild epithelial dysplasia (Fig. 4E). This is interesting, since Gata-3 has been shown to be involved in maintaining the differentiated state and is highly expressed in breast tumors of the luminal A subtype (Sorlie et al. 2003), which have a good prognosis. Thus, deletion of Zfp157 allows the survival of Gata-3-null cells, which can nevertheless differentiate. It may be concluded that Gata-3 is not essential for the differentiation or maintenance of alveolar cells and that the critical role of Gata-3, in concert with Stat6, is to suppress expression of Zfp157.

Id2 is a target of Zfp157

Since deletion of *zfp157* skews alveolar cells toward the pStat5 lineage, we investigated possible targets of Zfp157 that could account for the observed phenotype. A good candidate is Id2, which is regulated by Stat5a (Santos et al. 2010) and is essential for alveologenesis (Mori et al. 2000). Precocious up-regulation of Id2 expression and increased nuclear localization were apparent in *zfp157*$^{lacZ/LacZ}$ glands (Fig. 5A–C). Id proteins are thought to induce cell proliferation and negatively regulate differentiation, and *Id2*$^{-/-}$ mammary glands were observed to have defects in cell proliferation and survival (Mori et al. 2000). The early activation of Id2 seen in *zfp157*$^{lacZ/LacZ}$ glands resonates well with the observed increase in proliferation and may explain in part the survival of Gata-3-null cells. Id2 has recently been suggested to be a direct target of Stat5 in memory T cells (Yang et al. 2011), suggesting that it is the pStat5$^+$ cells that express Id2. Furthermore, RANKL has been reported to induce phosphorylation of Id2 at Ser 5, leading to nuclear retention, which is of itself sufficient to rescue the defective differentiation and cell death that occur in mammary glands from *RANKL*$^{-/-}$ mice (Kim et al. 2011). Setdb1, which is a histone H3 Lys 9 (H3K9)-specific methyltransferase, binds the promoter of Id2 and suppresses its expression through installing H3K9 methylation (Cho et al. 2011). Setdb1 associates with KAP-1 (which is a molecular scaffold for KRAB-ZFPs and therefore, presumably, Zfp157) to form heterochromatin and thereby repress expression of Zfp157 target genes.

We propose that the previously uncharacterized zinc finger protein Zfp157 is a master regulator of lineage determination during alveologenesis in mammary glands, where it maintains the balance of ERα/PR/Gata3-expressing cells and pStat5-expressing cells. Deletion of Zfp157 reveals the plasticity of alveolar progenitors and their complexity. In addition to the two previously identified lineages, we uncovered additional populations of alveolar cells.

Our findings provide new insights into the interactions between cells in the mammary gland and how hormone-sensing populations interact to control proliferation and function. Furthermore, we demonstrated that there are more than the two alveolar lineages previously identified. This is of interest in understanding the cell of origin of breast cancer. An important outcome of this work is the demonstration that subtle phenotypes in knockout mice may mask the true importance of a gene, which is revealed only by further gene deletion.

Materials and methods

Animals

Zfp157 knockout mice were generated using embryonic stem cells containing a LacZ gene inserted into the *zfp157* locus, obtained from BayGenomics. Chimeras were generated by morula injection into C57Bl/6 embryos by J. Nichols. Germline transmission was achieved, and heterozygous offspring were crossed to generate homozygotes. The mice were bred in regular cages in the animal facility of the Department of Pathology. The 8- to 10-wk-old virgin female mice were mated, the plug was checked to confirm mating, and pregnancy was confirmed post-mortem to avoid pseudo-pregnancies. Estrus was checked in the virgin mice. All animals were treated according to the local ethical committee and the UK Home Office guidelines.

Mammary gland whole mounts

The whole abdominal mammary gland (#4) was spread onto a glass slide, allowed to dry briefly, and subsequently incubated overnight in Carnoys fixative (60% ethanol [BDH], 30% chloroform [Fisher], 10% glacial acetic acid [Fisher]). The gland was then placed in carmine alum stain (1 g of carmine red [Sigma], 2.5 g of aluminium potassium sulphate [Sigma], 500 mL of dH_20) overnight. The tissue was destained in 70% ethanol and preserved in Histoclear II (National Diagnostics).

Tissue sections

Tissue for sectioning was collected from abdominal glands. The glands were fixed in 4% formaldehyde in PBS (Sigma) overnight at room temperature and, following fixation, stored in 70% ethanol (BDH) at −20°C until embedded. Tissues were embedded in wax and sectioned at 5-μm thickness onto a glass slide. For H&E staining, sections were dewaxed using xylene, rehydrated using an ethanol series, and then incubated in Harris' hemotoxylin solution for minutes. Sections were blued under running tap water and placed in eosin for 1 min. After washing, the sections were dehydrated in ethanol and xylene before mounting in DPX.

X-gal staining

The tissue was removed and fixed in 4% paraformaldehyde in PBS (pH 7.0–7.5) for 30 min to 1 h at 4°C with agitation. The samples were then washed three times for 30 min in rinse buffer (PBS at pH 7.3, 2 mM MgCl2, 0.01% sodium deoxycholate, 0.02% NP-40) at room temperature. After washing, the staining solution (rinse buffer, 5 mM potassium ferricyanide, 5 mM potassium ferrocyanide, 1 mg/mL X-gal) was added, and the samples were left for up to 48 h in the dark at 37°C. Tissues were post-fixed in 10% formalin in PBS at 4°C and cleared by dehydration in an ethanol series, followed by incubation in HistoClear II (National Diagnostics).

IF

Paraffin-embedded sections were deparaffnized in xylene by three separate 5-min washes. Sections were then rehydrated by 5-min washes in a serial ethanol series ending in dH_20 (100%, 90%, 70%, 50%, 30%). Antigen retrieval was carried out by incubating the slides under pressure in boiling 10 mM trisodium citrate buffer (pH 6.0) for 10 min, and then the slides were allowed to cool for 20 min. Sections were washed in ddH_20 for 5 min, dried, and circled with a PAP pen (Vector Laboratories). Sections were covered with the appropriate blocking solution and left in a humid chamber for 1 h at room temperature; then the blocking solution was removed and the primary antibody or an isotype control diluted in blocking buffer was applied and left overnight at 4°C in a humid chamber. Antibodies used were pStat5 (Cell Signaling, #9359), Gata-3 (Santa Cruz Biotechnology, sc-268), ERα (Santa Cruz Biotechnology, sc-542), Ki67 (Novocastra Laboratories, NCL-Ki67), PCNA (Santa Cruz Biotechnology, sc-56), and PR (Dako, A0098). Following incubation overnight, the sections were washed three times in PBS for 5 min each and incubated with a species-specific fluorescently labeled secondary antibody diluted 1:500 in blocking buffer in a humid chamber for 1 h at room temperature in the dark; the secondary antibody was removed and replaced by Bisbensimide-Hoechest 33342 (Sigma) for 5 min to stain the DNA. Subsequently, the sections were washed three times in PBS in the dark. Slides were mounted with a 1:1 PBS/glycerol solution and coverslip.

RNA extraction

Mammary tissue was collected, snap-frozen in liquid nitrogen, and then stored at −80°C. Tissue was ground using a mortar and pestle under liquid nitrogen. Forty milligrams of ground tissue was placed in an RNase-free 1.5-mL eppendorf tube, 1 mL of Trireagent (Sigma) was added, and a micropestle was used to disperse the tissue. The sample was then centrifuged at 11,000 rpm for 10 min at 4°C. The supernatant was collected in a fresh tube, and 200 μL of chloroform was added; the samples were shaken vigorously by hand and then left at room temperature for 3 min before centrifugation at 11,000 rpm for 15 min at 4°C, and the upper aqueous phase was transferred to a fresh tube. To precipitate the RNA, 500 μL of isopropanol was added and mixed by inversion, and the sample was incubated at room temperature for 10 min before being centrifuged at 11,000 rpm for 10 min at 4°C. The supernatant was discarded, and the pellet was resuspended in 700 μL of 70% ethanol. The RNeasy minikit (Qiagen) was used to isolate the RNA according to the manufacturer's instructions. RNA quality and concentration were ascertained using a Nanodrop ND-100 (Nanodrop Technologies).

cDNA

cDNA was made using SuperScript II reverse transcriptase kit (Invitrogen). One microgram of RNA was made up to 10 μL with ultrapure water (Sigma), incubated with 1 μL of random primers (Promega) and 1 μL of 10 mM dNTPs (Sigma) for 5 min at 65°C, and then placed on ice. One microliter of RNasin (Promega), 2 μL of 0.1 M DTT, and 4 μL of 5× first strand buffer were added to each sample. The samples were then incubated for 2 min at 25°C before 1 μL of SuperScript II reverse transcriptase was added. Samples were then incubated for 10 min at 25°C, 50 min at 42°C, and 15 min at 70°C. After incubation, the samples were made up to 50 μL with ultrapure water and stored at −20°C.

qRT–PCR

qRT–PCR was performed using 2 μL of cDNA, to which 10 μL of 2× SYBR green jump-start PCR master mix (Sigma) containing the taq enzyme, buffer, dNTPs, and SYBR green; 0.4 μL of each primer (10 μM); and 7.2 μL of ultrapure water (Sigma) were added. Cyclophilin A was used as an internal control. A Bio-Rad iCycler PCR machine with a halogen tungsten lamp was used, and data were analyzed using iCycler iQ software. Triplicates were run for each sample. Primers used for real-time PCR were designed using the PrimerBank Web site (http://pga.mgh.harvard.edu/primerbank) (Wang and Seed 2003). All primers were purchased from Sigma-Aldrich. The following primers were used: cyclophilin A (sense, 5′-CCTTGGGCCGCGTCTCCTT-3′; antisense, 5′-CACCCTGGCACATGAATCCTG-3′), genotyping (antisense, 5′-WTTGTCAGAGTGCCCAATCCTA-3′; antisense knockout, 5′-CCACAACGGGTTCTTCTGTT-3′; sense, 5′-GCCCCGTGATAAGTGTCATT-3′), Id2 (sense, 5′-ATGAAAGCCTTCAGTCCGTG-3′; antisense, 5′-AGCAGACTCATCGGGTCGT-3′), Zfp157 (exon 5) (sense 5′-ACTTCACTTGGCAGGAATGG-3′; antisense, 5′-GGAGACGCCAGACTGAAGTG-3′), and Zfp157 (sense, 5′-GGAACTTCCCCGAGGTACAAA-3′; antisense, 5′-GACATTCCTTCCATTCGTATGGT-3′).

Subcellular fractionation

To perform nuclear/cytoplasmic fractionation, 40 mg of ground, frozen mammary gland tissue was homogenized in 200 μL of buffer A (10 mM HEPES-potassium hydroxide at pH 7.9, 10 mM potassium chloride, 2 mM magnesium chloride, 0.5 mM DTT, 0.1 mM EDTA, 0.1 mM EGTA, 0.2 mM sodium fluoride, protease inhibitor cocktail [Roche]). Samples were incubated on ice for 15 min before 12.5 μL of buffer B (10% NP-40 in dH2 0) was added. Samples were vortexed for 15 sec and then centrifuged at 13,800*g* for 5 min at 4°C to pellet the nuclei. The supernatant was collected as the cytoplasmic fraction. The remaining pellet was resuspended in 50 μL of buffer C (50 mM HEPES-potassium hydroxide at pH 7.9, 50 mM potassium chloride, 300 mM sodium chloride, 1 mM DTT, 0.1 mM EDTA, 10% glycerol, 0.2 mM sodium orthovanadate, protease inhibitor cocktail [Roche]) and incubated for 20 min on ice with vortexing every 5 min. The samples were then centrifuged at 13,800*g* for 5 min at 4°C, and the supernatant was

collected as the nuclear fraction. Protein concentration was measured using bicinchoninic acid (BCA) protein concentration assay (Pierce) according to the manufacturer's instructions.

Western blotting

Protein samples were made up to a final concentration of normally 3 μg/μL using RIPA buffer and loading buffer (50 mM Tris, 10% glycerol, 2% SDS, 0.1% Bromophenol blue, 0.2% β-mercaptoethanol). The samples were boiled for 5 min at 95°C and then stored at −20°C. Resolving gels of the required acrylamide concentration were prepared and run on a miniprotean III Bio-Rad system. Proteins were immunoblotted onto PVDF membranes (Millipore, immobilon FL) using Bio-Rad wet transfer tanks. After immunoblotting, the PVDF membranes were incubated in blocking solution for 60 min and then diluted with primary antibody in blocking buffer overnight at 4°C. The membranes were rinsed once with 1× PBS-0.1% Tween20 (PBS-T) (Sigma). The appropriate secondary antibody was diluted to a final concentration of 1:2000 in the blocking buffer and incubated with the membrane for 45 min at room temperature. The secondary antibodies used were all conjugated with horseradish peroxidase (HRP) (DAKO). The membrane was then washed three times with 1× PBS-T for 5 min each. ECL (Amersham) was used according to the manufacturer's instructions, and chemiluminescence was detected using film (Konica Minolta). The antibodies used were Id2 (Santa Cruz Biotechnology, sc-489), Lamin A/C (Cell Signaling, #2032), Tubulin (Abcan ab6160), WAP (Santa Cruz Biotechnology, sc-14832), and pStat5 (Cell Signaling, #9359).

Generation of Zfp157-venus constructs

Full-length and truncated forms of Zfp157 were amplified using the following primers: full-length (Fwd, 5′-ATGGGGTTGGT GTCATTTGA-3′; Rev, 5′-GAGGATCCCCTGAGTTCATTCAC ATTGAA-3′), Krab domain (Fwd, 5′-ATGGGGTTGGTGTCA TTTGA-3′; Rev, 5′-GAGGATCCTGGGAGACGCCAGACTGA AGT-3′), and ZNF domain (Fwd, 5′-GTCGACATGGGTGTTC TTGAAGTTTATACT-3′; Rev, 5′-GAGGATCCCCTGAGTTCA TTCACATTGAA-3′). PCR products were sequence-verified and cloned in-frame with pVenus.

Primary mammary cell preparation and FACS analysis/cell sorting

Cells were isolated from mammary glands according to the protocol in Stingl et al. (2006). The primary antibodies used were biotinylated anti-CD45 (clone 30-F11, eBioscience), anti-Ter119 (clone Ter119, eBioscience), and anti-CD31 (clone 390, eBioscience); anti-CD24-R-phycoerythrin (PE; clone M1/69, eBioscience), anti-CD49f-Alexa Fluor 647 (AF647; clone GoH3, eBioscience), anti-CD49b-Alexa Fluor 488 (AF488; clone HMa2, eBioscience), anti-CD61-Alexa 488 (104311, BioLegend), and anti-Sca1-Alexa Fluor 647 (AF647; clone D7, eBioscience). The secondary antibodies used were Strepavidin-PE-Texas Red (PE-TR, Molecular Probes). Apoptotic cells were excluded by elimination of propidium iodide (PI)-positive cells. Flow cytometric analysis was done using CyAN ADP (DakoCytomation), and all sorts were performed using MoFlo (DakoCytomation); gates were set to exclude >99.9% of cells labeled with isoform-matched control antibodies conjugated with the corresponding fluorochromes.

Ma-CFC assay

Colony-forming assays were carried out as described in Stingl et al. (2006). The medium used was (human) NeuroCult NS-A proliferation medium (StemCell) supplemented with 5% FBS, 10 ng/mL epidermal growth factor (Sigma), 10 ng/mL basic fibroblast growth factor (Peprotech), and N2 Supplement (Invitrogen), and the cultures were maintained for 7 d at 37°C/5% CO_2, then fixed using ice-cold acetone:methanol (1:1) and visualized using Giemsa staining (Merck).

RNA extraction and real-time PCR analysis

RNA from sorted cells was extracted using PicoPure RNA isolation kit (Molecular Devices) according to the manufacturer's instructions.

In silico analysis and ChIP

In silico analysis and images of Stat6- and Gata-3-binding sites on the *Zfp157* locus were generated using the freeware Genepalette 1.2. Control or IL4-treated (50 ng/mL) (R&D systems) EpH4 cells were harvested, fixed, and lysed using ChIP-It Express kit (Active Motif) according to manufacturer's instructions. DNA sheering optimization was performed using a Bioruptor Next Gen sonicator (Diagenode). Antibody incubation was performed overnight at 4°C with the following antibodies: normal rabbit IgG (Cell Signaling, #2729), Stat6, Stat3, and Gata-3 (SCBT). qPCR was performed using 2 μL of purified input and pull-down DNA.

Probability calculations

The conditional probabilities shown in Figure 3 were performed by R. Thomas using Bayes' formula: $P(A|B) = P(A \cap B)/P(B)$. These probabilities represent the relative empirical frequency of Gata-3 in the presence of pStat5 and vice versa in control and knockout mice.

Statistical analysis

Statistical significance was assessed using unpaired two-tailed Student's *t*-tests in Microsoft Excel (TTEST). Standard deviations were also calculated using Microsoft Excel (STDEV).

Acknowledgments

We thank Dr. David Nelson for the pVenus expression plasmid, and Dr. William Paul for the Gata-3 floxed mice. C.H.O. was supported by a BBSRC PhD studentship. W.T.K. is funded by The Wellcome Trust, a BBSRC project grant, and a Junior Research Fellowship, King's College, Cambridge. H.T.F. is supported by a Wellcome Trust PhD studentship. This work was supported by BBSRC grant BB/H006206/1 to C.J.W. W.T.K. identified Zfp157 as a Stat6-regulated gene and carried out the cloning of Zfp157, ChIP analysis, FACS, and colony assays. J.N. injected blastocysts with the ES gene trap line XC356 and generated the Zfp157 reporter mice. C.H.O. carried out most of the remaining experiments except for the analysis of the Stat6 knockout mice and some IF studies, which were carried out by H.T.F. C.J.W. contributed to the design of the experiments, and C.H.O., W.T.K., and C.J.W. wrote the manuscript.

References

Asselin-Labat ML, Sutherland KD, Barker H, Thomas R, Shackleton M, Forrest NC, Hartley L, Robb L, Grosveld FG, van der Wees J, et al. 2007. Gata-3 is an essential regulator of mammary-gland morphogenesis and luminal-cell differentiation. *Nat Cell Biol* **9:** 201–209.

Booth BW, Smith GH. 2006. Estrogen receptor-α and progesterone receptor are expressed in label-retaining mammary

epithelial cells that divide asymmetrically and retain their template DNA strands. *Breast Cancer Res* **8:** R49. doi: 10.1186/bcr1538.

Cho S, Park JS, Kang YK. 2011. Dual functions of histone-lysine N-methyltransferase Setdb1 protein at promyelocytic leukemia-nuclear body (PML-NB): Maintaining PML-NB structure and regulating the expression of its associated genes. *J Biol Chem* **286:** 41115–41124.

Choi YS, Chakrabarti R, Escamilla-Hernandez R, Sinha S. 2009. Elf5 conditional knockout mice reveal its role as a master regulator in mammary alveolar development: Failure of Stat5 activation and functional differentiation in the absence of Elf5. *Dev Biol* **329:** 227–241.

Conneely OM, Mulac-Jericevic B, Arnett-Mansfield R. 2007. Progesterone signaling in mammary gland development. *Ernst Schering Found Symp Proc* **14:** 45–54.

Cui Y, Riedlinger G, Miyoshi K, Tang W, Li C, Deng CX, Robinson GW, Hennighausen L. 2004. Inactivation of Stat5 in mouse mammary epithelium during pregnancy reveals distinct functions in cell proliferation, survival, and differentiation. *Mol Cell Biol* **24:** 8037–8047.

He Z, Cai J, Lim JW, Kroll K, Ma L. 2011. A novel KRAB domain-containing zinc finger transcription factor ZNF431 directly represses Patched1 transcription. *J Biol Chem* **286:** 7279–7289.

Hennighausen L, Robinson GW. 2005. Information networks in the mammary gland. *Nat Rev Mol Cell Biol* **6:** 715–725.

Khaled WT, Read EK, Nicholson SE, Baxter FO, Brennan AJ, Came PJ, Sprigg N, McKenzie AN, Watson CJ. 2007. The IL-4/IL-13/Stat6 signalling pathway promotes luminal mammary epithelial cell development. *Development* **134:** 2739–2750.

Kim NS, Kim HJ, Koo BK, Kwon MC, Kim YW, Cho Y, Yokota Y, Penninger JM, Kong YY. 2006. Receptor activator of NF-κB ligand regulates the proliferation of mammary epithelial cells via Id2. *Mol Cell Biol* **26:** 1002–1013.

Kim NS, Kim HT, Kwon MC, Choi SW, Kim YY, Yoon KJ, Koo BK, Kong MP, Shin J, Cho Y, et al. 2011. Survival and differentiation of mammary epithelial cells in mammary gland development require nuclear retention of Id2 due to RANK signaling. *Mol Cell Biol* **31:** 4775–4788.

Kouros-Mehr H, Slorach EM, Sternlicht MD, Werb Z. 2006. GATA-3 maintains the differentiation of the luminal cell fate in the mammary gland. *Cell* **127:** 1041–1055.

Li W, Ferguson BJ, Khaled WT, Tevendale M, Stingl J, Poli V, Rich T, Salomoni P, Watson CJ. 2009. PML depletion disrupts normal mammary gland development and skews the composition of the mammary luminal cell progenitor pool. *Proc Natl Acad Sci* **106:** 4725–4730.

Liu X, Robinson GW, Wagner KU, Garrett L, Wynshaw-Boris A, Hennighausen L. 1997. Stat5a is mandatory for adult mammary gland development and lactogenesis. *Genes Dev* **11:** 179–186.

Liu X, Gallego MI, Smith GH, Robinson GW, Hennighausen L. 1998. Functional rescue of Stat5a-null mammary tissue through the activation of compensating signals including Stat5b. *Cell Growth Differ* **9:** 795–803.

Mehra R, Varambally S, Ding L, Shen R, Sabel MS, Ghosh D, Chinnaiyan AM, Kleer CG. 2005. Identification of GATA3 as a breast cancer prognostic marker by global gene expression meta-analysis. *Cancer Res* **65:** 11259–11264.

Miyoshi K, Shillingford JM, Smith GH, Grimm SL, Wagner KU, Oka T, Rosen JM, Robinson GW, Hennighausen L. 2001. Signal transducer and activator of transcription (Stat) 5 controls the proliferation and differentiation of mammary alveolar epithelium. *J Cell Biol* **155:** 531–542.

Mori S, Nishikawa SI, Yokota Y. 2000. Lactation defect in mice lacking the helix–loop–helix inhibitor Id2. *EMBO J* **19:** 5772–5781.

Oakes SR, Naylor MJ, Asselin-Labat ML, Blazek KD, Gardiner-Garden M, Hilton HN, Kazlauskas M, Pritchard MA, Chodosh LA, Pfeffer PL, et al. 2008. The Ets transcription factor Elf5 specifies mammary alveolar cell fate. *Genes Dev* **22:** 581–586.

Ray S, Dutta D, Rumi MA, Kent LN, Soares MJ, Paul S. 2009. Context-dependent function of regulatory elements and a switch in chromatin occupancy between GATA3 and GATA2 regulate Gata2 transcription during trophoblast differentiation. *J Biol Chem* **284:** 4978–4988.

Santos SJ, Haslam SZ, Conrad SE. 2010. Signal transducer and activator of transcription 5a mediates mammary ductal branching and proliferation in the nulliparous mouse. *Endocrinology* **151:** 2876–2885.

Shackleton M, Vaillant F, Simpson KJ, Stingl J, Smyth GK, Asselin-Labat ML, Wu L, Lindeman GJ, Visvader JE. 2006. Generation of a functional mammary gland from a single stem cell. *Nature* **439:** 84–88.

Skarnes WC, von Melchner H, Wurst W, Hicks G, Nord AS, Cox T, Young SG, Ruiz P, Soriano P, Tessier-Lavigne M, et al. 2004. A public gene trap resource for mouse functional genomics. *Nat Genet* **36:** 543–544.

Sorlie T, Tibshirani R, Parker J, Hastie T, Marron JS, Nobel A, Deng S, Johnsen H, Pesich R, Geisler S, et al. 2003. Repeated observation of breast tumor subtypes in independent gene expression data sets. *Proc Natl Acad Sci* **100:** 8418–8423.

Stingl J, Eirew P, Ricketson I, Shackleton M, Vaillant F, Choi D, Li HI, Eaves CJ. 2006. Purification and unique properties of mammary epithelial stem cells. *Nature* **439:** 993–997.

Takaki H, Ichiyama K, Koga K, Chinen T, Takaesu G, Sugiyama Y, Kato S, Yoshimura A, Kobayashi T. 2008. STAT6 Inhibits TGF-β1-mediated Foxp3 induction through direct binding to the Foxp3 promoter, which is reverted by retinoic acid receptor. *J Biol Chem* **283:** 14955–14962.

Urrutia R. 2003. KRAB-containing zinc-finger repressor proteins. *Genome Biol* **4:** 231. doi: 10.1186/gb-2003-4-10-231.

Wang X, Seed B. 2003. A PCR primer bank for quantitative gene expression analysis. *Nucleic Acids Res* **31:** e154. doi: 10.1093/nar/gng154.

Yamaji D, Na R, Feuermann Y, Pechhold S, Chen W, Robinson GW, Hennighausen L. 2009. Development of mammary luminal progenitor cells is controlled by the transcription factor STAT5A. *Genes Dev* **23:** 2382–2387.

Yang CY, Best JA, Knell J, Yang E, Sheridan AD, Jesionek AK, Li HS, Rivera RR, Lind KC, D'Cruz LM, et al. 2011. The transcriptional regulators Id2 and Id3 control the formation of distinct memory $CD8^+$ T cell subsets. *Nat Immunol* **12:** 1221–1229.